SIAM J. Applied Dynamical Systems
Vol. 10, No. 1, pp. 251–277

Smoke-Ring Solutions of Gierer–Meinhardt System in $\mathbb{R}^3$*

Theodore Kolokolnikov† and Xiaofeng Ren‡

Abstract. We consider the steady states of the Gierer–Meinhardt system on all of $\mathbb{R}^3$: $\varepsilon^2\Delta a - a + \frac{a^p}{h^q} = 0$, $\Delta h - h + \frac{a^m}{h^s} = 0$ with an additional restriction $q = p - 1$. In the limit $\varepsilon \to 0$, we use formal asymptotics to construct a solution whose activator component a concentrates on a circle. Under the additional constraints $p > 1$, $m > 0$, and $1 < m - s < 3$, we find that such a solution exists and is unique. The radius of the circle of concentration is given explicitly in terms of certain integrals. Full numerical computations are shown to support the analytical results.

Key words. smoke-ring solutions, Gierer–Meinhardt system, Green's functions

AMS subject classifications. 35Q92, 35B40, 35K57, 35J08

DOI. 10.1137/100802293

1. Introduction.

The fascinating smoke-ring structure has been observed in many physical systems. In [13] and [14], Malevanets and Kapral numerically observed stable links and knot structures in bistable chemical media (using particle simulation of the FitzHugh–Nagumo model), including linked smoke-rings. In fluid dynamics, a vortex ring is a region of a rotating fluid where the flow pattern takes on a toroidal shape [2]. In a quantum fluid, a vortex ring is formed by a loop of poloidal quantized flow pattern. It was detected in the superfluid helium by Rayfield and Reif [25] and more recently in Bose–Einstein condensates by Anderson et al. [1]. In block copolymers, Pochan et al. [22] produced a morphological phase of toroidal supramolecule assemblies using a triblock copolymer.

In this paper we study the smoke-ring structure in the classical Gierer–Meinhardt (GM) system on all of $\mathbb{R}^3$:

$$\varepsilon^2\Delta a - a + \frac{a^p}{h^q} = 0, \qquad \Delta h - h + \frac{a^m}{h^s} = 0, \tag{1.1}$$

where ε is a small positive parameter, $0 < \varepsilon \ll 1$, and

$$p, q, m, s \geq 0; \quad \frac{qm}{p-1} - s - 1 > 0. \tag{1.2}$$

The variable a is the activator and h is the inhibitor of the system. The goal of this paper is to construct a solution whose activator component concentrates on a circle as $\varepsilon \to 0$; this is schematically represented in Figure 1. More precisely, there is a circle in the xy-plane of

*Received by the editors July 15, 2010; accepted for publication (in revised form) by T. Kaper January 23, 2011; published electronically March 24, 2011.
http://www.siam.org/journals/siads/10-1/80229.html
†Department of Mathematics and Statistics, Dalhousie University, Halifax, Canada (tkolokol@mathstat.dal.ca). This author is supported by NSERC Discovery grant 47050.
‡Department of Mathematics, The George Washington University, Washington, DC (ren@gwu.edu). This author is supported in part by NSF grant DMS-0907777.

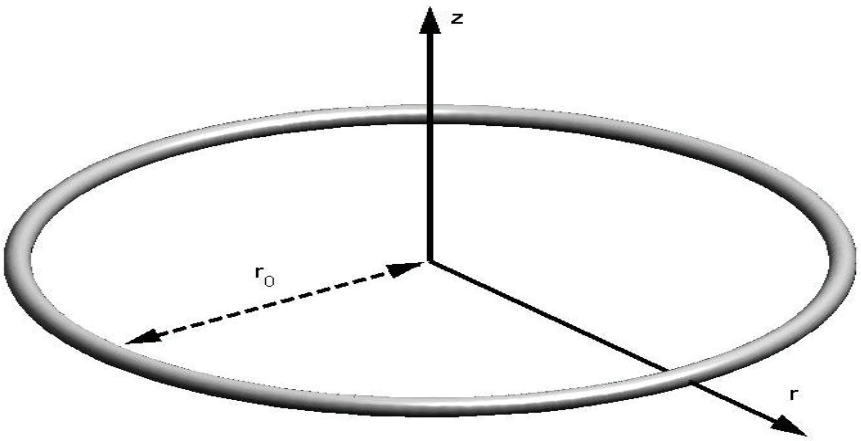

Figure 1. *Schematic representation of the smoke-ring solution in three dimensions. The gray region is a level set of the activator a, which is exponentially small everywhere except within an $O(\varepsilon)$ region of a circle of radius r_0.*

radius r_0 and a toroidal-shaped neighborhood of the circle in $\mathbb{R}^3$. Each cross section of the neighborhood, perpendicular to the circle, is a small disc whose radius is of order ε. The a variable of our solution is very small outside the toroidal neighborhood. Inside the neighborhood and on each cross section, a is almost a two-dimensional radially symmetric function with its maximum at the center. In $\mathbb{R}^3$ such a solution has an axisymmetry (cylindrical symmetry), so it is effectively a solution of a two-dimensional problem. We will refer to such a solution as a *smoke-ring solution*.

The problem (1.1) has a long history. It was introduced in [8] to model the head formation of a hydra. More generally, it can be used to study morphogenesis in cell development [15, 16, 19]. It is a minimal model that provides a theoretical bridge between observations on the one hand and the deduction of the underlying molecular-genetic mechanisms on the other. Mathematically, it is one of the simplest systems of PDEs that has a very rich solution structure and has been studied intensively over the last two decades. Let us highlight some of the results. In one dimension, there exist spike-like solutions whose activator component a concentrates at certain points and is exponentially small away from such points. While the solution with a single spike was shown to be stable in [29], multiple spike solutions exhibit intricate stability properties first shown in [6] by the matched asymptotics method; see also [26] for a related approach using Floquet exponents and Evans functions. In two dimensions, spike solutions, their stability, and their dynamics have also been studied; see, for example, [30, 31, 32, 28, 12] and references therein. Similar techniques have also been used to study spike solutions in other systems, such as the Gray–Scott model; see, for example, [3, 4, 5, 11, 18] and references therein.

On the other hand, little is known about the GM model in three or more dimensions. For example, the existence of a single spike solution on all of $\mathbb{R}^3$ is a long-standing open problem. The only result in three dimensions so far is the existence of the so-called ring solutions, in which the activator a concentrates on a two-dimensional sphere in $\mathbb{R}^3$ [20, 9].

Such solutions are radially symmetric; the activator variable a is (almost) a one-dimensional spike in the radial direction (analogous solutions for the Gray–Scott model have also been studied using similar techniques in [10] and [17]). On the contrary, the smoke-ring solution that we will construct concentrates on a one-dimensional circle. Unlike the ring solutions, the smoke-ring solution is *not radially symmetric but axisymmetric*; the cross-sectional profile of the activator a for a smoke-ring is (almost) a two-dimensional spike. To our knowledge, this is the first nonradial solution of the GM model in $\mathbb{R}^3$.

Related to the GM system (1.1) is the GM system with *saturation*:

$$\varepsilon^2 \Delta a - a + \frac{a^p}{(1+\kappa a^p)h^q} = 0, \qquad \Delta h - h + \frac{a^m}{h^s} = 0. \tag{1.3}$$

Note the saturation constant $\kappa > 0$ in (1.3). In [24] Ren and Wei studied a geometric problem that arises as a singular limit of (1.3). Solutions to their geometric problem are subsets of $\mathbb{R}^3$ that satisfy an equation involving the mean curvature and the Newtonian potential on the boundaries of the subsets. They found a solution shaped like a torus.

Since smoke-ring solutions have cylindrical symmetry, we rewrite (1.1) in cylindrical coordinates. Let $r = \sqrt{x_1^2 + x_2^2}$, $z = x_3$. We also rescale $a = \alpha u$, $h = \beta v$, where we take $\alpha = \left(\frac{\eta}{\varepsilon^2}\right)^{\frac{q}{(p-1)m(-1-s)}}$, $\beta = \alpha^{\frac{p-1}{q}}$ to put the system (1.1) in the form

$$\begin{cases} \varepsilon^2\left(\Delta_{(r,z)}u + \dfrac{1}{r}u_r\right) - u + \dfrac{u^p}{v^q} = 0, \\ \Delta_{(r,z)}v + \dfrac{1}{r}v_r - v + \dfrac{\eta}{\varepsilon^2}\dfrac{u^m}{v^s} = 0, \\ u_r(0,z) = v_r(0,z) = 0, \quad z \in \mathbb{R}, \\ u, v \to 0 \ \text{ as } |(r,z)| \to \infty, \end{cases} \quad (r,z) \in \mathbb{R}^2_+, \tag{1.4}$$

where $\Delta_{(r,z)} = \partial_{rr} + \partial_{zz}$, $\mathbb{R}^2_+ = (0,\infty) \times (-\infty, \infty)$, and

$$\eta = \frac{1}{\ln(1/\varepsilon)}. \tag{1.5}$$

The reason for using this scaling is that, as we will show later, $u, v = O(1)$ in the inner region of the spike. Equation (1.4) is our starting point. We now summarize the main result of this paper.

Main Result 1.1. *Consider the GM model (1.4) with $p > 1$, $m > 0$, and additional constraints*

$$p = q + 1 \tag{1.6}$$

and

$$1 < m - s < 3. \tag{1.7}$$

Then (1.4) admits a smoke-ring solution of the form

$$u(r,z) \sim Cw(R) + O\left(\frac{1}{\ln(1/\varepsilon)}\right) \quad \text{as } \varepsilon \to 0, \tag{1.8}$$

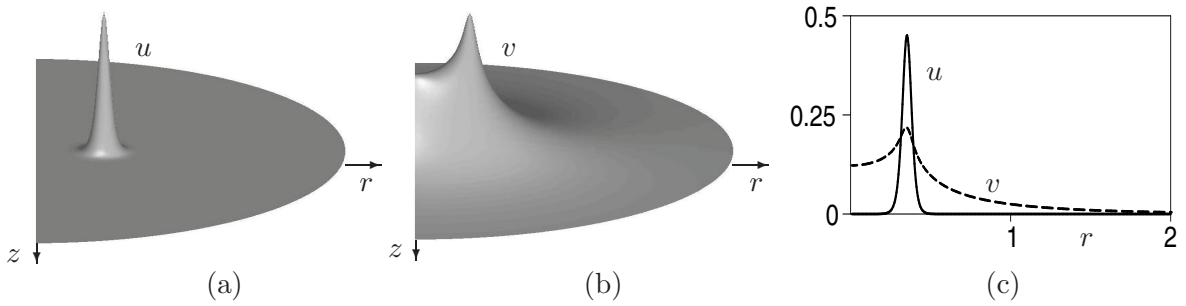

Figure 2. *A numerical solution of (1.4) showing a smoke-ring. The parameters are $\varepsilon = 0.02$, $p = 2$, $q = 1$, $m = 2$, $s = 0$. The computation was performed on a quarter-disk of radius 8; see section 4 for the details. An initial condition in the form of a smoke-ring was used. Here, the solution is shown with $z^2 + r^2 < 4$. (a) $u(x)$; (b) $v(x)$; (c) the cross-sections of u (solid curve) and v (dashed curve) along the r axis. The spike center is located at $r_0 = 0.353$, $z_0 = 0$.*

where C is some positive constant; $R = \frac{1}{\varepsilon}\sqrt{(r - r_0)^2 + z^2}$; w is the unique radially symmetric ground state solution in two dimensions that satisfies

$$\begin{cases} w_{RR} + \dfrac{1}{R} w_R - w + w^p = 0, \quad R \in (0, \infty), \\ w_R(0) = 0, \quad w \to 0 \text{ as } R \to \infty; \end{cases} \tag{1.9}$$

and r_0 is the asymptotic radius of the smoke-ring which satisfies the algebraic equation

$$1 - 2r_0 \int_0^1 \frac{e^{-2r_0 t}}{\sqrt{1 - t^2}} dt = \frac{1}{2}(m - s - 1) \frac{\int_0^\infty w^m \left(\int_0^R w^{p+1} t dt \right) R dR}{\left(\int_0^\infty w^m R dR \right) \left(\int_0^\infty w^{p+1} R dR \right)}. \tag{1.10}$$

The equation (1.10) has exactly one solution $r_0 > 0$ provided that (1.7) is satisfied.

Our analysis reveals a distinguished regime $p = q + 1$. In particular, the "standard" GM system $(p, q, m, s) = (2, 1, 2, 0)$ happens to satisfy this condition. For this case, Figure 2 shows the structure of the smoke-ring solution as obtained by solving (1.4) numerically with $\varepsilon = 0.02$; from such a solution, its radius was found to be $r_0 = 0.353$. On the other hand, solving (1.10) yields the asymptotic estimate $r_0 = 0.3279$, which is in good agreement with full numerics (see section 4 for further discussion of numerics).

The existence of smoke-ring solutions for the case $p \neq q + 1$ is an open problem. Based mainly on numerical experiments in section 4, we conjecture that they can still exist if $p < q+1$ but with radius $\varepsilon \ll r_0 \ll 1$.

We remark that the derivation of Main Result 1.1 is based on formal but very careful asymptotics. A rigorous derivation is not yet available (see section 5).

Our approach involves a mix of formal asymptotics as well as a careful study of a Green's function. The analysis is complicated by the presence of two scales, $O(\varepsilon)$ and $O(\frac{1}{\ln 1/\varepsilon})$. Moreover, the outer and inner regions of u interact in an intricate way, and a relatively high-order expansion is required.

We now summarize the contents of the paper. In section 2 we construct the inner and outer solutions and formulate the first-order solvability condition in order to determine the

smoke-ring radius r_0. Assuming $r_0 = O(1)$, it then becomes clear that in the case $p = q + 1$, a higher-order expansion is required (if $p \neq q + 1$, the first-order solvability condition will imply that r_0 cannot be of $O(1)$). This is done in section 3 and leads to the formula (1.10), which is the main result of this paper. In section 4 we show some numerical computations of the full two-dimensional system (1.4) and observe a favorable agreement with our analytical results. We also include some additional numerical experiments to speculate what happens when $p < q+1$ or $p > q+1$. Finally, we mention some related phenomena and open problems in section 5.

2. Preliminaries: Smoke-ring profile and the first-order solvability condition. In this section, we first construct the leading-order asymptotic profile of the smoke-ring equilibrium of a fixed radius r_0. We will then derive a solvability condition in an attempt to determine the value of r_0. This condition will yield the following dichotomy: either $p = q + 1$, in which case a higher-order expansion will be necessary to determine r_0, or else r_0 cannot be of $O(1)$. The case $p = q + 1$ will then be further analyzed in section 3, where a higher-order expansion will finally enable us to determine r_0. The derivation of the asymptotic profile and the first-order solvability condition is relatively standard; here we follow a procedure similar to that used in [12].

The exposition below is divided into three steps. In Step 1 we derive the leading-order asymptotic profile. The first-order solvability condition is derived in Step 2. Finally, in Step 3 we use Pohozhaev-type identities to simplify the resulting expression and identify the distinguished case $p = q + 1$.

Step 1. We begin by constructing the asymptotic profile of the smoke-ring solution. We seek a solution to (1.4) where $u(x)$ is assumed to concentrate at some point $x_0 = (r_0, z_0)$; that is, $u(x)$ is assumed to be very small everywhere except in a disc of radius $O(\varepsilon)$ centered at x_0. On the other hand, $v(x)$ will be nearly constant in the $O(\varepsilon)$ neighborhood of x_0. An example of such a solution is shown in Figure 2.

To simplify the notation, we define

$$g(u, v) := u^m v^{-s}, \quad h(v) := v^{-q}. \tag{2.1}$$

In the limit $\varepsilon \to 0$, we formally replace the nonlinearity in the second equation of (1.4) by a multiple of a delta function:

$$\frac{\eta}{\varepsilon^2} g(u, v) \sim C_0 \delta(x - x_0), \tag{2.2}$$

where $x = (r, z)$, $x_0 = (r_0, z_0)$,

$$C_0 := \int_{\mathbb{R}^2_+} \frac{\eta}{\varepsilon^2} g(u, v) dx,$$

and δ is the delta function. Here $\mathbb{R}^2_+ = \{(r, z) : r > 0,\ z \in \mathbb{R}\}$. Then in the outer region, i.e., when $|(r, z) - (r_0, z_0)| \gg O(\varepsilon)$, we estimate

$$v \sim C_0 G(r, z, r_0, z_0), \tag{2.3}$$

where G is a Green's function in the cylindrical coordinates that satisfies

$$\Delta_{(r,z)} G + \frac{1}{r} G_r - G = -\delta(x - x_0) \tag{2.4}$$

on all of $\mathbb{R}^2_+$. When matching with the inner region, we will need to know the behavior of G when x is near x_0. This behavior is summarized as follows.

Lemma 2.1. *Let $x_0 = (r_0, z_0)$, and let $x = x_0 + \varepsilon y$, where $y = (\rho, Z)$ and $\varepsilon \ll 1$. Let $\eta = 1/\ln(1/\varepsilon)$ be as in (1.5). Then*

$$2\pi\eta G(x, x_0) = 1 - \eta \ln|y| + \eta F_0(r_0) + \frac{\varepsilon\rho}{2r_0}\left(-1 + \eta\left(\ln|y| + F_1(r_0)\right)\right) + O(\varepsilon^2), \tag{2.5}$$

where

$$F_0(r_0) = \int_0^1 \left(\frac{1}{\tau}\frac{\exp(-2r_0\tau)}{\sqrt{1-\tau^2}} - \frac{1}{\tau}\right) d\tau + \ln 4r_0, \tag{2.6}$$

$$F_1(r_0) = -F_0(r_0) + r_0 F_0'(r_0). \tag{2.7}$$

The proof of Lemma 2.1 is given in Appendix A.

Next we examine the profile of the solution inside the smoke-ring. By symmetry, we may assume that $z_0 = 0$. Near the center $x_0 = (r_0, 0)$, we define the inner variable as

$$y = \frac{x - x_0}{\varepsilon} \tag{2.8}$$

and let

$$R = |y|, \quad y = (\rho, Z). \tag{2.9}$$

Using Lemma 2.1, we rewrite the outer solution (2.3) in terms of inner variables (2.8) to obtain

$$v \sim \xi\left[1 - \eta\ln R + \eta F_0(r_0) + \frac{\varepsilon\rho}{2r_0}\left(-1 + \eta\ln R + \eta F_1(r_0)\right)\right], \quad |y| \to \infty, \tag{2.10}$$

where F_0, F_1 are given in Lemma 2.1. Here, ξ is given by

$$2\pi\xi = \int_{\mathbb{R}^2_+} \frac{g(u,v)}{\varepsilon^2} dx.$$

Next we examine the profile of the solution in the inner region, near x_0. We define the inner variables U and V by

$$u(x) = U(y), \quad v(x) = V(y), \tag{2.11}$$

where, as in (2.8), $x = x_0 + \varepsilon y$. Then (1.4) becomes

$$\begin{cases} \Delta_y U + \dfrac{\varepsilon}{\rho + \varepsilon r_0} U_\rho - U + U^p h(V) = 0, \\ \Delta_y V + \dfrac{\varepsilon}{\rho + \varepsilon r_0} V_\rho - \varepsilon^2 U + \eta g(U, V) = 0. \end{cases} \tag{2.12}$$

Since the problem contains two scales $\varepsilon \ll \eta \ll 1$, we first expand (2.12) in terms of ε while treating η as a constant. We use the following expansion:

$$\begin{aligned} U(y) &= U_0(R) + \varepsilon U_1(y) + \cdots, \\ V(y) &= V_0(R) + \varepsilon V_1(y) + \cdots, \\ \xi &= \xi_0 + \varepsilon\xi_1 + \cdots. \end{aligned}$$

The $O(1)$-order equations are

$$\begin{aligned} \Delta_y U_0 - U_0 + U_0^p h(V_0) &= 0, \\ \Delta_y V_0 + \eta g(U_0, V_0) &= 0, \\ \xi_0 = \textstyle\int_0^\infty g(U_0, V_0) R dR. & \end{aligned} \tag{2.13}$$

The solutions U_0 and V_0 are both radially symmetric. Next we expand in η,

$$U_0 = U_{00} + \eta U_{01} + \dots, \quad V_0 = V_{00} + \eta V_{01} + \dots, \quad \xi_0 = \xi_{00} + \eta \xi_{01} + \dots, \tag{2.14}$$

to obtain

$$\xi_{00} = \int_0^\infty g R dR, \tag{2.15}$$

$$V_{00} = \xi_{00}, \tag{2.16}$$

$$\Delta_y U_{00} - U_{00} + h U_{00}^p = 0. \tag{2.17}$$

Here and below, we omit the arguments of $h = h(\xi_{00})$ and $g = g(U_{00}, \xi_{00})$. From (2.17) we deduce

$$U_{00}(y) = h^{\frac{1}{1-p}} w(R),$$

where w is the radial ground state solution of $\Delta_y w - w + w^p = 0$ in $\mathbb{R}^2$, i.e.,

$$w_{RR} + \frac{1}{R} w_R - w + w^p = 0, \quad w_R(0) = 0, \quad \lim_{R \to \infty} w(R) = 0.$$

For the GM model this yields

$$\xi_{00}^{1+s-\frac{mq}{p-1}} = \left(\int_0^\infty w^m R dR \right). \tag{2.18}$$

This computation shows that the leading-order profile of the smoke-ring is given by (1.8); the precise value of the constant C in (1.8) is $C = \xi_{00}^{\frac{1}{1-p}}$ with ξ_{00} given by (2.18).

Step 2. At this stage, the smoke-ring radius r_0 is undetermined. It is therefore necessary to consider the higher-order expansion to determine it.

To this end, we collect the $O(\varepsilon)$ terms in (2.12), which yield

$$\Delta_y U_1 + \frac{1}{r_0} U_{0\rho} + (-1 + p h(V_0) U_0^{p-1}) U_1 + h_v(V_0) U_0^p V_1 = 0, \tag{2.19}$$

$$\Delta_y V_1 + \frac{1}{r_0} V_{0\rho} + (g_u(U_0, V_0) U_1 + g_v(U_0, V_0) V_1)\, \eta = 0. \tag{2.20}$$

We now expand the $O(\varepsilon)$ equations in terms of η. We write

$$U_1 = U_{10} + \eta U_{11} + \cdots, \quad V_1 = V_{10} + \eta V_{11} + \cdots, \quad \xi_1 = \xi_{10} + \eta \xi_{11} + \cdots \tag{2.21}$$

and define

$$L\Phi \equiv \Delta_y \Phi + \left(-1 + p h U_{00}^{p-1} \right) \Phi = \Delta_y \Phi + \left(-1 + p w^{p-1} \right) \Phi. \tag{2.22}$$

We deduce

$$L(U_{10}) = -h_v U_{00}^p V_{10} - \frac{1}{r_0} U_{00\rho}, \tag{2.23}$$

$$\Delta_y V_{10} = 0, \tag{2.24}$$

where $h_v = h_v(\xi_{00})$. The first-order solvability condition is obtained by multiplying (2.19) by $U_{00\rho}$ and integrating by parts. Noting that $U_{00\rho}$ satisfies $L(U_{00\rho}) = 0$, we obtain

$$\int_{\mathbb{R}^2} \frac{1}{r_0} U_{00\rho}^2 dy + \int_{\mathbb{R}^2} h_v U_{00}^p U_{00\rho} V_{10} dy = 0. \tag{2.25}$$

To determine V_{10}, we invoke Van Dyke's matching principle [27]. That is, we expand the outer solution $v(x)$ in terms of the inner variables (2.8) and then match it to the inner solution V. Since we seek to determine V_{10}, we must expand $v(x)$ up to $O(\varepsilon)$. Starting with (2.10), we have

$$v \sim \xi \left[1 - \eta \ln R + \eta F_0(r_0) + \frac{\varepsilon \rho}{2 r_0} \left(-1 + \eta \ln R + \eta F_1(r_0) \right) + O\left(\varepsilon^2\right) \right], \quad 1 \ll |y| \ll \frac{1}{\varepsilon}, \tag{2.26}$$

$$\sim \xi_{00} + O(\eta) + \varepsilon \left(-\frac{\rho \xi_{00}}{2 r_0} + O\left(\eta\right) \right) + O(\varepsilon^2). \tag{2.27}$$

Matching the $O(\varepsilon^1 \eta^0)$ terms in (2.27) with the behavior of V_{10} for large y, we obtain that $V_{10} \sim -\frac{\xi_{00}\rho}{2r_0}$ as $y \to \infty$. In conjunction with (2.24) this implies that

$$V_{10} = -\frac{\xi_{00}\rho}{2r_0} + C$$

for some constant C. Therefore, (2.25) becomes

$$\int_{\mathbb{R}^2} U_{00\rho}^2 dy - \frac{\xi_{00}}{2} h_v \int_{\mathbb{R}^2} U_{00}^p U_{00\rho} \rho dy = 0. \tag{2.28}$$

Step 3. We now simplify the solvability condition (2.28). Note that

$$\int_{\mathbb{R}^2} U_{00\rho}^2 = \pi \int_0^\infty U_{00R}^2 R dR, \qquad \int_{\mathbb{R}^2} U_{00}^p U_{00\rho} \rho = -\pi \frac{2}{p+1} \int_0^\infty U_{00}^{p+1} R dR. \tag{2.29}$$

Next we use Pohozhaev-type identities; see, for example, [23] or [28]. Multiplying (2.17) by U_{00} and integrating by parts, we obtain

$$-\int_0^\infty U_{00R}^2 R dR - \int_0^\infty U_{00}^2 R dR + h \int_0^\infty U_{00}^{p+1} R dR = 0. \tag{2.30}$$

Multiplying (2.17) by $U_{00R} R$ and integrating by parts, we obtain

$$\int_0^\infty U_{00}^2 R dR = \frac{2}{p+1} h \int_0^\infty U_{00}^{p+1} R dR \tag{2.31}$$

so that

$$\int_0^\infty U_{00R}^2 R dR = \frac{p-1}{p+1} h \int_0^\infty U_{00}^{p+1} R dR. \tag{2.32}$$

Substituting (2.29)–(2.32) into (2.28), we find

$$\left(p - 1 + \frac{\xi_{00} h_v}{h}\right) \frac{\pi}{4r_0} \int_0^\infty U_{00}^2 R dR = 0. \tag{2.33}$$

From (2.1), we have $\frac{\xi_{00} h_v}{h} = -q$, so that (2.33) becomes

$$(p - 1 - q) \int_0^\infty U_{00}^2 R dR = 0. \tag{2.34}$$

If $p - 1 \neq q$, then the condition (2.34) simply states that no smoke-ring of radius $O(1)$ can exist in the limit $\varepsilon \to 0$. On the other hand, if $p - 1 = q$, then the condition (2.34) cannot determine the value of r_0, and a deeper expansion is necessary. This is the subject of the next section.

3. The case $p = q + 1$. We now consider the distinguished regime $p = q + 1$. In this section we will show that in this case, the smoke-ring radius is given by (1.10), which is the main result of the paper. When $p = q + 1$, the first-order solvability condition (2.34) is $0 = 0$, and hence a deeper expansion is required to determine r_0. The derivation is very involved, but, unexpectedly, there are many cancellations so that the end-result is surprisingly simple.

We break the computations of this section into three steps. In Step 1, we compute the $O(\eta)$ and $O(\varepsilon\eta)$ corrections to $U(y)$ and $V(y)$ (refer to section 2 for notation). In Step 2, we formulate the solvability condition at the $O(\varepsilon\eta)$th order. In Step 3, we explore some identities to significantly simplify the solvability condition and to finally obtain (1.10).

Step 1. In this step we derive the expressions for the inner solution, up to order $O(\varepsilon\eta)$. These expressions will play a key role in formulating and simplifying the solvability condition of Step 2.

We start by computing the $O(\eta)$ terms U_{01}, V_{01}, and ξ_{01} in (2.14). The $O(\eta)$ terms in (2.13) yield

$$L U_{01} + U_{00}^p h_v V_{01} = 0, \tag{3.1}$$

$$\Delta_y V_{01} + g = 0, \tag{3.2}$$

$$\xi_{01} = \int_0^\infty g_u U_{01} R dR + \int_0^\infty g_v V_{01} R dR. \tag{3.3}$$

Here $h_v = h_v(\xi_{00})$, $g_u = g_u(U_{00}, \xi_{00})$, $g_v = g_v(U_{00}, \xi_{00})$, and L is defined in (2.22). Integrating (3.2), we have

$$V_{01R} = -\frac{1}{R} \int_0^R g R dR \tag{3.4}$$

so that

$$V_{01} = g_1(R) + c_1, \quad \text{where} \quad g_1(R) := \int_0^R \frac{-1}{t} \int_0^t g(U_{00}, \xi_{00}) s ds \tag{3.5}$$

and c_1 is some constant that will be determined as follows. Expanding $g_1(R)$ asymptotically for large R and using the fact that $g(U_{00}, \xi_{00})$ decays exponentially as $R \to \infty$, we obtain

$$g_1(R) \sim -\ln(R) \int_0^\infty gsds + \int_0^\infty \ln(s) gsds, \quad R \to \infty, \tag{3.6}$$

$$V_{01} \sim -\xi_{00} \ln R + \int_0^\infty \ln(s) gsds + c_1, \quad R \to \infty. \tag{3.7}$$

To determine c_1, we match the $O(\eta)$th order of the inner and outer expansions. Substituting $\xi = \xi_{00} + \eta\xi_{01}$ into (2.10), and collecting the $O(\varepsilon^0)$ terms, we obtain

$$\begin{aligned} v &\sim (\xi_{00} + \eta\xi_{01}) \left[1 - \eta \ln R + \eta F_0(r_0)\right] \\ &\sim \xi_{00} - \eta\xi_{00} \ln R + \eta \left(\xi_{00} F_0(r_0) + \xi_{01}\right). \end{aligned} \tag{3.8}$$

Matching the behavior of the inner solution $V(R)$ as $R \to \infty$ (3.7) to that of the outer solution $v(x)$ as $x \to x_0$ (3.8), we obtain

$$c_1 = \xi_{00} F_0 + \xi_{01} + \alpha_1, \quad \text{where} \quad \alpha_1 = -\int_0^\infty \ln(s)\, gsds. \tag{3.9}$$

Next we determine ξ_{01}. We will make use of the identity

$$LU_{00} = (p-1)\, hU_{00}^p$$

so that $L^{-1}(U_{00}^p) = \frac{1}{(p-1)h} U_{00}$. We rewrite (3.1) as $U_{01} = L^{-1}\left(-h_v U_0^p V_{01}\right)$, and using (3.5), we obtain

$$\begin{aligned} U_{01} = L^{-1}\left(-h_v U_0^p V_{01}\right) &= h_v L^{-1}\left[g_1(R) U_0^p\right] - c_1 h_v L^{-1}\left[U_0^p\right] \\ &= h_v L^{-1}\left[g_1(R) U_0^p\right] - c_1 \frac{1}{p-1} \frac{h_v}{h} U_{00} \end{aligned}$$

so that

$$\int_0^\infty g_u U_{01} R dR = -c_1 \frac{1}{p-1} \frac{h_v}{h} \int_0^\infty g_u U_{00} R dR + \alpha_2, \tag{3.10}$$

$$\int_0^\infty g_v V_{01} R dR = c_1 \int_0^\infty g_v R dR + \alpha_3, \tag{3.11}$$

where

$$\alpha_2 := \int_0^\infty g_u h_v L^{-1}\left[g_1(R) U_0^p\right] R dR, \quad \alpha_3 := \int_0^\infty g_v \left(-\xi_{00} \ln R + \int_0^R \ln s gsds\right) R dR$$

are $O(1)$-order constants that are independent of r_0. Substituting (3.10)–(3.11) into (3.3) and replacing c_1 by (3.9), we obtain

$$\begin{aligned} \xi_{01} &= c_1 \beta + \alpha_2 + \alpha_3 \\ &= \left(\xi_{00} F_0(r_0) + \xi_{01} + \alpha_1\right) \beta + \alpha_2 + \alpha_3, \end{aligned}$$

where

$$\beta = \left(-\frac{1}{p-1}\frac{h_v}{h}\int_0^\infty g_u U_{00} R dR + \int_0^\infty g_v R dR \right). \tag{3.12}$$

Solving for ξ_{01}, we obtain

$$\xi_{01} = \xi_{00}\left(\frac{\beta}{1-\beta}F_0(r_0) + \alpha_5\right), \tag{3.13}$$

where

$$\alpha_5 := \frac{1}{\xi_{00}}\frac{\alpha_1\beta + \alpha_2 + \alpha_3}{1-\beta}$$

is an $O(1)$-order constant independent of r_0.

From (2.1) we have $g_u U_{00} = mg$, $g_v\xi_{00} = -sg$, and $h_v\xi_{00} = -qh$, and recalling (2.15), we deduce

$$\beta = \frac{qm}{p-1} - s = m - s. \tag{3.14}$$

Next, we compute the behavior of V_1 for large y to two orders. To do this, we expand the outer solution $v(x)$ in terms of the inner variables (2.8). Starting with (2.10), we have

$$\begin{aligned}
v &\sim \xi\left[1 - \eta\ln R + \eta F_0(r_0) + \frac{\varepsilon\rho}{2r_0}\left(-1 + \eta\ln R + \eta F_1(r_0)\right)\right], \quad |y|\to\infty,\\
&\sim \xi_{00}\left[1 - \eta\ln R + \eta\left(F_0 + \frac{\xi_{01}}{\xi_{00}}\right) + \frac{\varepsilon\rho}{2r_0}\left(-1 + \eta\left\{\ln R + F_1(r_0) - \frac{\xi_{01}}{\xi_{00}}\right\}\right)\right]\\
&\quad + \varepsilon\xi_1\left(1 - \eta\ln R + \eta F_0(r_0)\right)\\
&\sim \xi_{00}\left[1 - \eta\ln R + \eta\left(\frac{1}{1-\beta}F_0(r_0) + \alpha_5\right)\right]\\
&\quad + \frac{\varepsilon\rho\xi_{00}}{2r_0}\left(-1 + \eta\left\{\ln R + F_1(r_0) - \frac{\beta}{1-\beta}F_0(r_0) - \alpha_5\right\}\right)\\
&\quad + \xi_{10}\varepsilon + \varepsilon\eta\xi_{10}\left(-\ln R + F_0(r_0)\right) + \varepsilon\eta\xi_{11}.
\end{aligned} \tag{3.15}$$

Matching the $O(\varepsilon)$ terms, we obtain

$$V_1 \sim \frac{\xi_{00}\rho}{2r_0}\left(-1 + \eta\left\{\ln R + F(r_0)\right\}\right) + \xi_{10} + \eta F_2(R, r_0), \quad |y|\to\infty, \tag{3.16}$$

where

$$F(r_0) := F_1(r_0) - \frac{\beta}{1-\beta}F_0(r_0) - \alpha_5, \qquad F_2(R, r_0) := \xi_{10}\left(-\ln R + F_0(r_0)\right) + \xi_{11}. \tag{3.17}$$

Step 2. We now formulate the main solvability condition for r_0. We anticipate that $r_0 = O(1)$, and, with (3.16) in mind, we make a change of variables

$$V_1 := \hat{V} + \frac{\xi_{00}\rho}{2r_0}\left(-1 + \eta\ln R + \eta F(r_0)\right) + \xi_{10} + \eta F_2(R, r_0).$$

Matching with the outer solution, we then note that

$$\hat{V} = O\left(\frac{1}{|y|}\right) \quad \text{as } |y| \to \infty.$$

To formulate a higher-order solvability condition, we use the idea introduced in [12] to rewrite $O(\varepsilon)$-order equations as a system. Let

$$W := \begin{bmatrix} U_1 \\ \hat{V} \end{bmatrix}.$$

Since

$$\Delta_y (\rho \ln R) = \frac{2\cos\theta}{R},$$

(2.19)–(2.20) become

$$\Delta_y W + MW = K \tag{3.18}$$

in the matrix form where

$$M = \begin{bmatrix} -1 + phU_0^{p-1} & h_v U_0^p \\ \eta g_u & \eta g_v \end{bmatrix}, \tag{3.19}$$

$$K = \frac{1}{r_0}\begin{bmatrix} -U_{0\rho} - h_v U_0^p \left[\frac{\xi_{00}\rho}{2}(-1 + \eta \ln R + \eta F(r_0)) + r_0\xi_{10} + \eta r_0 F_2(R, r_0)\right] \\ -V_{0\rho} - \eta\xi_{00}\frac{\cos\theta}{R} + \frac{\xi_{00}\rho}{2}\eta g_v + O(\eta^2) \end{bmatrix}. \tag{3.20}$$

Now let $\Psi = [N, P]$ be the solution to the adjoint system

$$\Delta_y \Psi + \Psi M = 0.$$

The solvability condition is formulated by multiplying (3.18) by Ψ on the left, integrating over a big ball $B = \{y : |y| < R\}$, and then letting $R \to \infty$. We obtain

$$\int_{\partial B} (\Psi \partial_n W - \partial_n \Psi W)\, dS(y) = \int_B \Psi K\, dy.$$

Write $\Psi = [N, P]$ and expand in η:

$$\begin{aligned} \Psi &= \Psi_0 + \eta\Psi_1 + \cdots, \\ N &= N_0 + \eta N_1 + \cdots, \\ P &= P_0 + \eta P_1 + \cdots. \end{aligned}$$

In addition, expand

$$U_1 = U_{10} + \eta U_{11}, \quad V_1 = V_{10} + \eta V_{11}.$$

The equation for N_0 then becomes

$$\Delta_y N_0 + N_0 (-1 + hU_{00}^p) = 0,$$

which admits a solution

$$N_0 = \partial_\rho U_{00}.$$

Since U decays exponentially at infinity and $\hat{V} \sim O(1/|y|)$ for large $|y|$, we find that for a sufficiently large ball B,

$$\int_{\partial B} (\Psi \partial_n W - \partial_n \Psi W)\, dS(y) \sim 0.$$

Next we evaluate $\int_B \Psi K$. At the leading order, we estimate $V_{0\rho} \sim 0$, $U_0 \sim U_{00}$ so that

$$0 = \int_B \Psi K\, dy = \frac{1}{r_0} \int_{\mathbb{R}^2} \left(-U_{00\rho}^2 + h_v \xi_{00} U_{00}^p \rho U_{00\rho}\right) dy + O(\eta).$$

Using integration by parts, the identity (2.32), and, by assumption, $p = q - 1$, this integral is zero. Therefore, to determine r_0 it is necessary to look at $O(\eta)$-order terms. The full expansion is

$$\begin{aligned} 0 &= \int_B \Psi K dy \\ &\sim \eta \frac{1}{r_0} \int_{\mathbb{R}^2} \begin{pmatrix} \left(-U_{00\rho} + \frac{\xi_{00}}{2} h_v \rho U_{00}^p + r_0 \xi_{10}\right) N_1 - U_{00\rho} U_{01\rho} \\ + \frac{\xi_{00}}{2} h_v p U_{00}^{p-1} \rho U_{00\rho} U_{01} + \frac{\xi_{00}}{2} h_{vv} U_{00}^p \rho U_{00\rho} V_{01} \\ -h_v U_{00}^p \left[\frac{\xi_{00}\rho}{2} (\ln R + F(r_0)) + r_0 F_2(R, r_0)\right] U_{00\rho} \\ + \left(-V_{01\rho} - \xi_{00} \frac{\cos\theta}{R} + \xi_{00} \frac{\rho}{2} g_v\right) P_0 \end{pmatrix} dy + O(\eta^2). \end{aligned} \tag{3.21}$$

At first sight, this looks daunting. However, surprisingly, there are hidden identities that greatly simplify this expression, as we now show.

Step 3. We start with equations for N_1 and P_0 which are

$$\Delta_y N_1 + N_1 \left(-1 + p h U_{00}^{p-1}\right) + U_{00\rho} \left(p(p-1) h U_{00}^{p-2} U_{01} + p h_v U_{00}^{p-1} V_{01}\right) + g_u P_0 = 0; \tag{3.22}$$

$$\Delta_y P_0 + h_v U_{00}^p \partial_\rho U_{00} = 0. \tag{3.23}$$

We will now make use of (3.22) to derive an additional identity and eliminate N_1 from (3.21). To do this, multiply (3.22) by ρU_{00} and integrate. First note that

$$\begin{aligned} \int_{\mathbb{R}^2} \Delta_y N_1 U_{00} \rho dy &= \int_{\mathbb{R}^2} N_1 \Delta_y (U_{00}\rho)\, dy \\ &= \int_{\mathbb{R}^2} N_1 \cos\theta \left(R \left(U_{00RR} + \frac{U_{00R}}{R}\right) + 2U_{00R}\right) dy \\ &= \int_{\mathbb{R}^2} N_1 \left(\rho (U_{00} - h U_{00}^p) + 2U_{00\rho}\right) dy \end{aligned}$$

so that

$$\int_{\mathbb{R}^2} \begin{Bmatrix} \left[2U_{00\rho} + ((p-1) h \rho U_{00}^p)\right] N_1 \\ + U_{00\rho} \left(p(p-1) h \rho U_{00}^{p-1} U_{01} + p h_v \rho U_{00}^p V_{01}\right) + g_u P_0 \rho U_{00} \end{Bmatrix} dy = 0. \tag{3.24}$$

Using $\xi_{00}h_{vv} = -(q+1)h_v$ as well as $p = q+1$, we then obtain

$$\begin{aligned}
&2\int_{\mathbb{R}^2}\left\{\left(-U_{00\rho}+\frac{\xi_{00}}{2}h_v\rho U_{00}^p\right)N_1+\frac{\xi_{00}}{2}h_v pU_{00}^{p-1}\rho U_{00\rho}U_{01}+\frac{\xi_{00}}{2}h_{vv}U_{00}^p\rho U_{00\rho}V_{01}\right\}dy\\
&=\int_{\mathbb{R}^2}\left\{\left(-2U_{00\rho}-(p-1)h\rho U_{00}^p\right)N_1-(p-1)hpU_{00}^{p-1}\rho U_{00\rho}U_{01}-ph_vU_{00}^p\rho U_{00\rho}V_{01}\right\}dy\\
&=\int_{\mathbb{R}^2}g_uP_0\rho U_{00}dy.
\end{aligned}$$

Also, by parity we have

$$\int_{\mathbb{R}^2}h_vU_{00}^pU_{00\rho}F_2(R,r_0)dy=0,\qquad \int_{\mathbb{R}^2}N_1dy=0.$$

Therefore, (3.21) simplifies to

$$0=\int_{\mathbb{R}^2}\left\{\begin{array}{l}-U_{00\rho}U_{01\rho}-h_vU_{00}^pU_{00\rho}\frac{\xi_{00}\rho}{2}\left(\ln R+F(r_0)\right)\\+\left(-V_{01\rho}-\xi_{00}\frac{\cos\theta}{R}+\xi_{00}\frac{\rho}{2}g_v+\frac{\rho}{2}g_uU_{00}\right)P_0\end{array}\right\}dy. \tag{3.25}$$

Next we write (3.25) as $I_1+I_2+I_3+I_4=0$, where

$$\begin{aligned}
I_1&=\int_{\mathbb{R}^2}-U_{00\rho}U_{01\rho}dy,\\
I_2&=\int_{\mathbb{R}^2}-h_vU_{00}^pU_{00\rho}\frac{\xi_{00}\rho}{2}\left(\ln R+F(r_0)\right)dy,\\
I_3&=\int_{\mathbb{R}^2}\left(-V_{01\rho}-\xi_{00}\frac{\cos\theta}{R}\right)P_0dy,\\
I_4&=\int_{\mathbb{R}^2}\left(\xi_{00}\frac{\rho}{2}g_v+\frac{\rho}{2}g_uU_{00}\right)P_0dy.
\end{aligned}$$

To simplify I_1 we will make use of the identity

$$L\left(U_{00R}R\right)=2(U_{00}-U_{00}^ph),$$

where L is the linear operator defined in (2.22). We have

$$\begin{aligned}
I_1&=-\int_{\mathbb{R}^2}U_{00\rho}U_{01\rho}dy=-\pi\int_0^\infty U_{00R}U_{01R}RdR=\pi\int_0^\infty U_{01}\left(U_{00}-hU_{00}^p\right)RdR\\
&=\pi/2\int_0^\infty L\left(U_{00R}R\right)RU_{01}dR=\pi/2\int_0^\infty U_{00R}L(U_{01})R^2dR\\
&=-\pi/2\int_0^\infty\left(h_vU_{00}^pV_{01}\right)U_{00R}R^2dR\\
&=\pi\int_0^\infty\frac{h_v}{p+1}U_{00}^{p+1}(V_{01}R+V_{01R}R^2/2)dR.
\end{aligned}$$

Next we evaluate I_3. First note that the solution to (3.23) is given explicitly by

$$P_0=-\frac{\cos\theta}{R}\frac{h_v}{p+1}\left(\int_0^R U_{00}^{p+1}(s)sds\right) \tag{3.26}$$

so that

$$\begin{aligned} I_3 &= -\int_{\mathbb{R}^2} \left(V_{01\rho} + \xi_{00} \frac{\cos\theta}{R} \right) P_0 dy \\ &= \pi \int_0^\infty \left(V_{01R} + \xi_{00} \frac{1}{R} \right) \frac{h_v}{p+1} \left(\int_0^R U_{00}^{p+1}(s) s ds \right) dR \\ &= \pi \lim_{t\to\infty} \left(V_{01}(t) + \xi_{00} \ln(t) \right) \frac{h_v}{p+1} \left(\int_0^\infty U_{00}^{p+1}(s) s ds \right) \\ &\quad - \pi \int_0^\infty \frac{h_v U_0^{p+1}}{p+1} \left(V_{01} + \xi_{00} \ln(R) \right) R dR. \end{aligned}$$

By (3.7), (3.9), and (3.13) we observe that

$$V_{01}(R) \sim \xi_{00} \left(-\ln R + \frac{1}{1-\beta} F_0(r_0) + \alpha_5 \right), \quad R \to \infty,$$

so that I_3 becomes

$$\begin{aligned} I_3 &= \pi \xi_{00} \left(\frac{1}{1-\beta} F_0(r_0) + \alpha_5 \right) \frac{h_v}{p+1} \left(\int_0^\infty U_{00}^{p+1}(s) s ds \right) \\ &\quad - \pi \int_0^\infty \frac{h_v}{p+1} U_0^{p+1} \left(V_{01} + \xi_{00} \ln(t) \right) R dR. \end{aligned}$$

Next we compute

$$\begin{aligned} I_2 &= \int_{\mathbb{R}^2} -h_v U_{00}^p U_{00\rho} \frac{\xi_{00}\rho}{2} \left(\ln R + F(r_0) \right) dy \\ &= \pi \int_0^\infty -h_v U_{00}^p U_{00R} \frac{\xi_{00}}{2} \left(\ln R + F(r_0) \right) R^2 dR \\ &= \pi \int_0^\infty \frac{h_v}{p+1} U_{00}^{p+1} \xi_{00} \left(\ln R + F(r_0) + 1/2 \right) R dR \\ &= \pi \int_0^\infty \frac{h_v}{p+1} U_{00}^{p+1} \xi_{00} \left(\ln R + F_1(r_0) - \frac{\beta}{1-\beta} F_0(r_0) - \alpha_5 + 1/2 \right) R dR. \end{aligned}$$

When combining $I_1 + I_2 + I_3$, we get to cancel many terms and obtain

$$I_1 + I_2 + I_3 = \pi \int_0^\infty \frac{h_v}{p+1} U_{00}^{p+1} (V_{01R} R/2 + \xi_{00} \left(F_1(r_0) + F_0(r_0) + 1/2 \right)) R dR.$$

Next we assume $g(u,v) = u^m v^{-s}$. Using $g_u U_{00} = mg$ and $g_v \xi_{00} = -sg$, we simplify

$$I_4 = -\frac{h_v}{p+1} \frac{\pi}{2} (m-s) \int_0^\infty gR \left(\int_0^R U_{00}^{p+1}(s) s ds \right) dR.$$

Moreover, recall from (3.4) that $gR = (-V_{01R} R)_R$ so that integrating by parts yields

$$\begin{aligned} I_4 &= -\frac{h_v}{p+1} \frac{\pi}{2} (m-s) \left\{ \lim_{R\to\infty} \left(-V_{01R} R \int_0^R U_{00}^{p+1}(s) s ds \right) + \int_0^\infty U_{00}^{p+1} V_{01R} R^2 dR \right\} \\ &= -\frac{h_v}{p+1} \frac{\pi}{2} (m-s) \left\{ \xi_{00} \left(\int_0^\infty U_{00}^{p+1}(s) R dR \right) + \int_0^\infty U_{00}^{p+1} V_{01R} R^2 dR \right\}. \end{aligned}$$

Hence the solvability condition $I_1 + I_2 + I_3 + I_4 = 0$ becomes

(3.27)
$$\frac{1-m+s}{2}\int_0^\infty U_{00}^{p+1} V_{01R} R^2 dR + \int_0^\infty U_{00}^{p+1}\xi_{00}\left(F_1(r_0)+F_0(r_0)+\frac{1-m+s}{2}\right) RdR = 0,$$

or, in a simpler form,

$$F_1(r_0)+F_0(r_0) = \frac{1}{2}(m-s-1)\left(1+\frac{\int_0^\infty U_{00}^{p+1}V_{01R}R^2dR}{\int_0^\infty U_{00}^{p+1}\xi_{00}RdR}\right). \tag{3.28}$$

Using (3.4) and (2.15), we obtain

$$\begin{aligned} 1+\frac{\int_0^\infty U_{00}^{p+1}V_{01R}R^2dR}{\int_0^\infty U_{00}^{p+1}\xi_{00}RdR} &= 1-\frac{\int_0^\infty w^{p+1}\left(\int_0^R w^m t dt\right)RdR}{\left(\int_0^\infty w^{p+1}RdR\right)\left(\int_0^\infty w^m RdR\right)} \\ &= \frac{\int_0^\infty w^m\left(\int_0^R w^{p+1}tdt\right)RdR}{\left(\int_0^\infty w^m RdR\right)\left(\int_0^\infty w^{p+1}RdR\right)}. \end{aligned} \tag{3.29}$$

Finally, using (2.6)–(2.7), we have

$$F_1(r_0)+F_0(r_0) = 1-2r_0\int_0^1 \frac{e^{-2r_0\tau}}{\sqrt{1-\tau^2}}d\tau. \tag{3.30}$$

Substituting (3.29) and (3.30) into (3.28), we obtain

$$1-2r_0\int_0^1\frac{e^{-2r_0\tau}}{\sqrt{1-\tau^2}}d\tau = \frac{1}{2}(m-s-1)\frac{\int_0^\infty w^m\left(\int_0^R w^{p+1}tdt\right)RdR}{\left(\int_0^\infty w^m RdR\right)\left(\int_0^\infty w^{p+1}RdR\right)},$$

which is precisely the formula (1.10). To complete the derivation of Main Result 1.1, it remains to prove the existence and uniqueness of the solution to the algebraic equation (1.10). This is done in Appendix B. The derivation of Main Result 1.1 is then complete.

4. Numerical experiments. To validate our analytical results and explore what happens if $p \neq q+1$, we used FlexPDE software [7] to compute the full two-dimensional smoke-ring solution of (1.4).

Experiment 1: $p = q+1$, *effect of* ε. We first consider the "standard" parameter values, $(p,q,m,s) = (2,1,2,0)$. This satisfies the condition $p = q+1$ of Main Result 1.1. We used Maple to compute the theoretically predicted value of r_0 by numerically solving (1.10) as follows. First, we used Maple's boundary value problem solver to determine the steady state w numerically. The integrals in (1.10) are then easily evaluated using Maple's numerical integrator. We found that the right-hand side of (1.10) is equal to 0.307043; the solution to (1.10) is given by $r_0 = 0.327929$. We then used FlexPDE to compute a fully two-dimensional smoke-ring–type steady state solution of (1.4) numerically for several different values of ε. We solved (1.4) on a quarter-disk of radius 8. Due to the presence of the logarithmic scaling, a very high error tolerance was required in order to achieve good convergence. For example, when we

took $\varepsilon = 0.02$, the numerical solution and the corresponding center of the spike r_0 appeared to change as the tolerance was slowly decreased even with relatively strict error tolerance; it finally settled for global error tolerances smaller than 5e-5. Fortunately, FlexPDE uses automatic adaptive gridding and was able to handle such tight tolerance. Using the tolerance of 5e-6 required about 4500 gridpoints (with most of the gridpoints concentrated near the spike) and yielded the numerical value of $r_0 = 0.3537$. The resulting solution is shown in Figure 2. This agrees well with the theoretical prediction (relative error about 7.9%). Table 1 shows the computation for several different values of ε.

Table 1

$(p, q, m, s) = (2, 1, 2, 0)$			
ε	r_0 using (1.4)	r_0 from (1.10)	%error
0.02	0.353170	0.327929	7.70%
0.04	0.377903	”	15.22%
0.08	0.450895	”	37.50%
0.025	0.357921	”	9.15%
0.05	0.394113	”	20.18%

It appears from the table that the error is of $O(\varepsilon)$ order: doubling ε appears to roughly double the error.

Table 2

$(p, q, m) = (2, 1, 2)$, $\varepsilon = 0.04$			
s	r_0 using (1.4)	r_0 from (1.10)	difference
-0.5000	0.293970	0.226969	0.067001
-0.3750	0.312172	0.249738	0.062434
-0.2500	0.332351	0.273998	0.058353
-0.1250	0.354415	0.299970	0.054445
0.0000	0.378852	0.327930	0.050922
0.1250	0.405267	0.358231	0.047036
0.2500	0.435668	0.391330	0.044338
0.3750	0.469093	0.427841	0.041252
0.5000	0.508206	0.468612	0.039594
0.6250	0.541612	0.514871	0.026741

Experiment 2: $p = q+1$, *effect of* s. We fix $(p, q, m) = (2, 1, 2)$ and $\varepsilon = 0.04$, and we vary s. As in Experiment 1, the asymptotic radius r_0 is given by (1.10), which is solved numerically for a given s. We then compare r_0 given by (1.10) with the numerical value computed using FlexPDE. We obtain Table 2; see also Figure 3(a). A clear agreement is observed between the analytical and numerical results. Also a good agreement is observed even with $s < 0$. Indeed, while s is usually taken to be positive, nothing in our analysis prevents it from being negative as long as (1.7) is satisfied.

Experiment 3: $q > p - 1$, *effect of* q. We take $(p, m, s) = (2, 2, 0)$ and $\varepsilon = 0.04$ and slowly increase q from 1. Computing the corresponding r_0 numerically, we obtain Table 3 (see also Figure 3(b)). The smoke-ring appears to exist for $1 \le q < 1.5$ until eventually r_0 becomes zero, at which point the smoke-ring becomes a three-dimensional spike.

Experiment 4: $q > p - 1$, *effect of* ε. We take $(p, m, s) = (2, 2, 0)$ and $q = 1.2$ and vary ε.

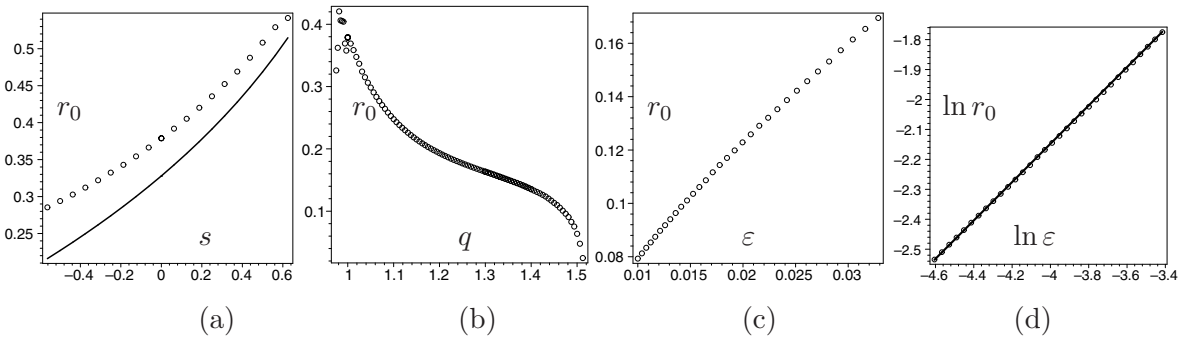

Figure 3. *Experiment* 2: *The effect of parameter* s *on the smoke-ring radius with* $(p, q, m) = (2, 1, 2)$ *and* $\varepsilon = 0.04$. *Dots indicate the radius obtained with direct numerical computation of* (1.4) *using FlexPDE. The solid line is obtained by solving for* r_0 *from formula* (1.10). (b) *Experiment* 3: *The effect of* q *with* $(p, m, s) = (2, 2, 0)$ *and* $\varepsilon = 0.04$. *A smoke-ring solution exists for* $1 < q < 1.5$. *For* $0.97 < q < 1$, *FlexPDE has a hard time converging and the solution seems to jump around; FlexPDE fails to converge when* $q \le 0.97$. (c) *Experiment* 4: *The effect of* ε *with* $(p, m, s) = (2, 2, 0)$ *and* $q = 1.2$. (d) *Experiment* 4 *on a log-log plot. The data is shown by circles; the line shows a straight-line fit* $r_0 \approx 1.51\varepsilon^{0.64}$ *through the last two points of the data.*

Table 3

$(p, m, s) = (2, 2, 0)$, $\varepsilon = 0.04$	
q	r_0 using (1.4)
1.000000	0.378721
1.050000	0.298360
1.100000	0.247756
1.150000	0.215230
1.200000	0.193186
1.250000	0.176765
1.300000	0.163324
1.350000	0.150154
1.400000	0.135573
1.450000	0.113338
1.500000	0.063746
1.55	0

Table 4

$(p, q, m, s) = (2, 1.2, 2, 0)$	
ε	r_0 using (1.4)
0.030432	0.161432
0.029286	0.157386
0.025119	0.142218
0.019953	0.122872
0.015252	0.103564
0.013082	0.094056
0.011659	0.087490
0.010000	0.079302

We then obtain Table 4 (see also Figure 3(c,d)). It is clear that unlike the case $p = q+1$, here we have $r_0 \to 0$ as $\varepsilon \to 0$. In Figure 3(d) we plot $\ln r_0$ versus $\ln \varepsilon$. The resulting plot looks like a straight line. Using the last two points of the table above, we numerically estimate that

$r_0 \sim 1.51\varepsilon^{0.64}$. It remains an open problem to determine the precise nature of such a small smoke-ring solution.

Experiment 5: $q < p-1$. We take $(p,m,s) = (2,2,0)$ and $\varepsilon = 0.04$ and attempt to compute r_0 with $q < 1$. We set the error tolerance to 10^{-5} and slowly decrease q below 1. *FlexPDE failed to converge to a solution even when* $q = 0.97$. For $q \in (0.98, 1]$, FlexPDE gave seemingly discontinuous values for r_0 as q was slowly decreased, as Table 5 demonstrates.

Table 5

$(p,m,s) = (2,2,0)$, $\varepsilon = 0.04$	
q	r_0 using (1.4)
1	0.378721
0.996875	0.357755
0.993750	0.369243
0.990625	0.404194
0.987500	0.405338
0.984375	0.406227
0.981250	0.420731
0.978125	0.362330
0.975000	0.325908
0.971875	failure to converge

Based on these numerical experiments, we conjecture that the smoke-ring solution does not exist when $q < p-1$.

5. Discussion. In this paper, we used formal asymptotics to construct smoke-ring solutions when $p-1 = q$. This may be viewed as a first step toward a more rigorous proof, which remains an open problem. The main obstacle in making our results rigorous is the presence of two scales, ε and $\log\varepsilon$, which require a double expansion and make it hard to apply standard rigorous techniques, such as Liapunov–Schmidt reduction, directly. In addition, a rigorous proof usually requires error estimates, so even higher-order expansions are required. This appears to be a formidable challenge, given that simply computing the radius r_0 required a manipulation of more than 10 terms (see (3.21)).

An outstanding open problem is the possible existence of the smoke-ring solutions when $p-1 \neq q$. From section 2, it is clear that in such a case, the radius cannot be $O(1)$, since this would contradict (2.34). However, we do not rule out the possible existence of smoke-rings of either a large radius, or a small radius of size $\varepsilon \ll r_0 \ll 1$. Indeed, the numerics of section 4 suggest the latter is possible for the case $q > p-1$. However, so far, we were unable to construct such a solution analytically.

Let us contrast the results of this paper to the radially symmetric solutions in three dimensions which concentrate on a sphere. Those were studied in [20] and [9]. It was found that such a solution exists provided that $q/2 < p-1 < q$. In this case, the radius of the sphere was found to be of order $O(1)$, independent of m, s; moreover, it satisfies

$$\frac{p-1}{q} = \frac{e^{2r_0} - 1 - r_0}{e^{2r_0} - 1}.$$

It is clear that r_0 becomes large as $p \to q+1$ from the left. By contrast, the smoke-ring solutions of radius $r_0 = O(1)$ exist when $p = q+1$. Numerical simulations of section 4 also

indicate that a smoke-ring solution may exist when $p < q + 1$; however, in this case the radius appears to be small. In addition, the smoke-ring radius also depends on m, s. An open question is whether a solution concentrating on a large sphere can exist in the borderline case $p = q + 1$.

It is unclear what happens if the condition (1.7) is violated, since neither existence nor uniqueness of a solution to (1.10) can be guaranteed in such a case. In particular, the shape of the left-hand side of (1.10) (see Figure 4) indicates that a multiplicity of smoke-ring solutions should be possible if $m-s-1$ is just slightly below zero, although eventually all such solutions disappear if $m-s-1$ is too negative. On the other hand, the smoke-ring solution will eventually disappear if s is sufficiently decreased so that the right-hand side of (1.7) exceeds 1; however, this generally happens when $m - s - 1 > 3$. In other words, the sufficient condition (1.7) is clearly not necessary for the existence of a smoke-ring solution.

An open (and difficult) question is to elucidate any connections between various types of solutions. For example, numerical simulations show that a ring solution in two dimensions connects to a spike solution as ε increases to $O(1)$. Such a connection is related to pattern-forming instabilities in one dimension: a two-dimensional spike can become unstable and expand into a hollow sphere. As the sphere radius is increased, it also becomes unstable and breaks up into spots. We speculate that in three dimensions, a spike can bifurcate into either a smoke-ring or a sphere when $p \le q + 1$.

The stability of smoke-ring solutions is also an open question. In two dimensions, it is known that a ring solution whose radius is of $O(1)$ is unstable and breaks up into spots; see, for example, [17, 10]. We therefore anticipate that the smoke-ring solution we constructed will be unstable with respect to angular perturbations when $p = q+1$. By contrast, numerical simulations indicate that a smoke-ring with *small* radius may exist when $p < q + 1$. It is unclear whether such a solution may be stable.

It would be interesting to study smoke-ring solutions on bounded domains. While Green's function for a general bounded domain is difficult, it may be possible to compute it for a special case of a three-dimensional ball. In particular, is $p = q + 1$ still an essential condition on a bounded domain? Some numerical simulations (not shown here) on a ball domain and with $(p, q, m, s) = (2, 1, 2, 0)$ suggest that the smoke-ring solution disappears as the domain radius is decreased below 2.

Appendix A. Proof of Lemma 2.1.

Step 1. The Green's function (2.4) has an integral representation that can be constructed as follows. Let $\Gamma(X, X_0)$ be the entire-space Green's function in three dimensions satisfying

$$\Delta_X \Gamma - \Gamma = -\delta(X - X_0), \quad X, X_0 \in \mathbb{R}^3.$$

Explicitly we have

$$\Gamma(X, X_0) = \frac{e^{-|X-X_0|}}{4\pi|X - X_0|}.$$

Now (2.4) can be trivially extended to three dimensions by letting $r = \sqrt{X_1^2 + X_2^2}$, $z = X_3$. It follows that G is the convolution of Γ with the circle of delta functions of radius r_0 (more precisely, with the one-dimensional Hausdorff measure restricted on the circle). This yields

an integral representation of G,

$$G(r,z,r_0,z_0)=\frac{r_0}{4\pi}\int_0^{2\pi}\frac{\exp[-(r^2+r_0^2-2rr_0\cos\omega+(z-z_0)^2)^{1/2}]}{(r^2+r_0^2-2rr_0\cos\omega+(z-z_0)^2)^{1/2}}\,d\omega. \tag{A.1}$$

We rewrite this as

$$G=\frac{r_0}{2\pi}\int_0^{\pi}\frac{\exp\{-[2rr_0(1-\cos\theta)+(r-r_0)^2+(z-z_0)^2]^{1/2}\}}{[2rr_0(1-\cos\theta)+(r-r_0)^2+(z-z_0)^2]^{1/2}}\,d\theta$$

and make a change of variables,

$$s=[2rr_0(1-\cos\theta)+(r-r_0)^2+(z-z_0)^2]^{1/2}. \tag{A.2}$$

After some simplifications we obtain

$$G=\frac{r_0e^{-\beta}}{\pi(\alpha-\beta)}\int_0^1\frac{\exp[-(\alpha-\beta)\tau]\,d\tau}{\sqrt{\tau(\delta+\tau)(1+\delta+\tau)(1-\tau)}},\quad\text{where} \tag{A.3}$$

$$\beta=[(r-r_0)^2+(z-z_0)^2]^{1/2},\quad \alpha=[(r+r_0)^2+(z-z_0)^2]^{1/2},\ \delta=\frac{2\beta}{\alpha-\beta}. \tag{A.4}$$

Now we write $x=x_0+\varepsilon y$, where $y=(\rho,Z)$, so that

$$r=r_0+\varepsilon\rho,\quad z=z_0+\varepsilon Z.$$

Then we have

$$\beta=\varepsilon\,|y|\,,\quad \alpha=2r_0+\varepsilon\rho+O(\varepsilon^2),\quad \delta=\frac{\varepsilon\,|y|}{r_0}\left(1-\frac{\varepsilon}{2r_0}\,(\rho-|y|)\right),\quad \alpha-\beta=2r_0+\varepsilon\,(\rho-|y|)$$

and

$$G=\frac{r_0e^{-\varepsilon|y|}}{\pi(2r_0+\varepsilon\,(\rho-|y|))}I(2r_0+\varepsilon\,(\rho-|y|)\,;\delta), \tag{A.5}$$

where

$$I\,(a,\delta):=\int_0^1\frac{\exp[-a\tau]\,d\tau}{\sqrt{\tau(\delta+\tau)(1+\delta+\tau)(1-\tau)}}. \tag{A.6}$$

Step 2. In this step we derive the following estimate of (A.6):

$$\begin{aligned}I(a,\delta)\sim{}&\ln\frac{1}{\delta}+2\ln 2+g_1(a)\\&+\delta\left\{(-1+a)\,\frac{1}{2}\ln\frac{1}{\delta}+(a-1)\left(\ln 2-\frac{1}{2}\right)+g_2(a)\right\}+O(\delta^2\ln\delta),\end{aligned} \tag{A.7}$$

where

$$g_1(a):=\int_0^1\left(\frac{\exp(-a\tau)}{\tau\sqrt{1-\tau^2}}-\frac{1}{\tau}\right)d\tau, \tag{A.8}$$

$$g_2(a):=\int_0^1\left(\frac{-2\tau-1}{2\tau^2(\tau+1)\sqrt{1-\tau^2}}\exp(-a\tau)+\frac{1}{2\tau^2}-\left(\frac{a}{2}-\frac{1}{2}\right)\frac{1}{\tau}\right)d\tau. \tag{A.9}$$

Note that the integral (A.6) becomes singular near $\tau = 0$ as $\delta \to 0$. We therefore choose γ with

$$\delta \ll \gamma \ll 1$$

and split $I = \int_0^\gamma + \int_\gamma^1 = I_1 + I_2$. To determine I_1, we rescale

$$\tau = \delta y$$

so that

$$I_1 = \int_0^{\gamma/\delta} \frac{\exp(-a\delta y)dy}{\sqrt{y\,(y+1)\,(1+\delta(y+1))\,(1-\delta y)}}.$$

Next we expand the integrand in terms of δ:

$$\frac{\exp(-a\delta y)dy}{\sqrt{y\,(y+1)\,(1+\delta(y+1))\,(1-\delta y)}} = \frac{1}{\sqrt{y(1+y)}} + \delta\frac{\left(-ay-\frac{1}{2}\right)}{\sqrt{y(1+y)}} + O(\delta^2).$$

Note that

$$\int_0^y \frac{1}{\sqrt{y(1+y)}}dy = 2\ln(\sqrt{y}+\sqrt{y+1}),$$
$$\int_0^y \frac{y}{\sqrt{y(1+y)}}dy = \sqrt{y(1+y)} - \ln(\sqrt{y}+\sqrt{y+1})$$

so that

$$I_1 = 2\ln(\sqrt{y}+\sqrt{y+1}) + \delta\left\{(-1+a)\ln(\sqrt{y}+\sqrt{y+1}) - a\left(\sqrt{y(1+y)}\right)\right\}, \quad y = \frac{\gamma}{\delta}.$$

Now, in the limit $y \to \infty$, we have

$$\ln(\sqrt{y}+\sqrt{y+1}) \sim \frac{1}{2}\ln y + \ln 2 + \frac{1}{4y} + O\left(\frac{1}{y^2}\right), \quad y \to \infty,$$

and

$$\sqrt{y(1+y)} \sim y + \frac{1}{2} - \frac{1}{8y} + O\left(\frac{1}{y^2}\right).$$

So we obtain

$$I_1 \sim \ln\frac{\gamma}{\delta} + 2\ln 2 + \frac{\delta}{2\gamma} + \delta\left\{(-1+a)\frac{1}{2}\ln\frac{\gamma}{\delta} - \ln 2 + a\left(\ln 2 - \frac{1}{2}\right)\right\} + O\left(\frac{\delta^2}{\gamma^2}\right) + O\left(\frac{\delta^2}{\gamma}\right) + O(\gamma). \tag{A.10}$$

In the end, all the γ terms should cancel with the γ terms coming from I_2. To compute I_2, expand

$$\begin{aligned} I_2 &= \int_\gamma^1 \frac{\exp(-a\tau)d\tau}{\sqrt{\tau\,(\tau+\delta)\,(\tau+1+\delta)\,(1-\tau)}} \\ &\sim \int_\gamma^1 \frac{\exp(-a\tau)d\tau}{\tau\sqrt{1-\tau^2}} + \delta\int_\gamma^1 \frac{-2\tau-1}{2\tau^2(\tau+1)\sqrt{1-\tau^2}}\exp(-a\tau)d\tau \\ &= I_{21} + \delta I_{22}. \end{aligned}$$

To find I_{21}, we note that the integrand behaves like τ^{-1} for small τ. We therefore rewrite

$$I_{21} = -\ln\gamma + g_1(a) + O(\gamma), \tag{A.11}$$

where g_1 is given in (A.8). Note that g_1 is a nonsingular integral that is independent of γ. To determine the $O(\delta)$ terms, we need to extract the singularity from I_{22}. Note that for small τ we have

$$\frac{-2\tau-1}{2\tau^2(\tau+1)\sqrt{1-\tau^2}}\exp(-a\tau)d\tau \sim -\frac{1}{2\tau^2} + \left(\frac{a}{2}-\frac{1}{2}\right)\frac{1}{\tau} + O(1), \quad \tau \to 0.$$

Therefore, we may write

$$I_{22} \sim \frac{1}{2}\left(1-\frac{1}{\gamma}\right) + \left(-\frac{a}{2}+\frac{1}{2}\right)\ln\gamma + g_2(a) + O(\gamma), \tag{A.12}$$

where g_2 is given by (A.9). The integrals g_1 and g_2 are nonsingular and can be easily evaluated numerically. Combining (A.11), (A.12), and (A.10), we note that $O(\ln\gamma)$- and $O\left(\delta\gamma^{-1}\right)$-order terms cancel out as expected, and we get (A.7).

Step 3. Recall that we have

$$a = 2r_0 + \varepsilon(\rho - |y|), \quad \delta = \frac{\varepsilon|y|}{r_0}\left(1 - \frac{\varepsilon}{2r_0}(\rho-|y|)\right),$$

so using (A.7) we obtain

$$\begin{aligned} I(a,\delta) &\sim \ln\frac{r_0}{\varepsilon|y|} + \frac{\varepsilon}{2r_0}(\rho-|y|) + 2\ln 2 + g_1(2r_0) + \varepsilon(\rho-|y|)g_1'(2r_0) \\ &\quad + \frac{\varepsilon|y|}{r_0}\left\{(-1+2r_0)\frac{1}{2}\ln\frac{r_0}{\varepsilon|y|} + (2r_0-1)\left(\ln 2 - \frac{1}{2}\right) + g_2(2r_0)\right\} + O(\varepsilon^2\ln\varepsilon) \\ &\sim \ln\frac{r_0}{\varepsilon|y|} + 2\ln 2 + g_1(2r_0) \\ &\quad + \varepsilon\left\{\begin{array}{c} \frac{1}{2r_0}(\rho-|y|) + |y|\left(-\frac{1}{2r_0}+1\right)\left(\ln\frac{r_0}{\varepsilon|y|} - 1 + 2\ln 2\right) \\ +\frac{|y|}{r_0}g_2(2r_0) + (\rho-|y|)g_1'(2r_0) \end{array}\right\} + O(\varepsilon^2\ln\varepsilon). \end{aligned} \tag{A.13}$$

We also expand

$$\frac{r_0 e^{-\varepsilon|y|}}{\pi(2r_0+\varepsilon(\rho-|y|))} \sim \frac{1}{2\pi}\left(1+\varepsilon\left(\frac{|y|-\rho}{2r_0} - |y|\right)\right). \tag{A.14}$$

Substituting (A.13)–(A.14) into (A.5), after some algebra we find

$$\begin{aligned} 2\pi G &\sim \ln\frac{r_0}{\varepsilon|y|} + 2\ln 2 + g_1(2r_0) \\ &\quad + \varepsilon\left\{\begin{array}{c} -\frac{\rho}{2r_0}\ln\frac{1}{\varepsilon} + \frac{\rho}{2r_0}\left\{\ln|y| - \ln r_0 - 2\ln 2 - g_1(2r_0) + 1 + 2r_0 g_1'(2r_0)\right\} \\ +\frac{|y|}{2r_0}\left\{(g_1(2r_0)+1)(1-2r_0) + 2g_2(2r_0) - 2r_0 g_1'(2r_0) - 1\right\} \end{array}\right\}. \end{aligned} \tag{A.15}$$

Step 4. To complete the proof, we claim that

$$2g_2(z) = (g_1(z)+1)(z-1) - zg_1'(z) + 1 \tag{A.16}$$

so that (A.15) simplifies to

$$\begin{aligned} 2\pi G \sim{}& \ln\frac{r_0}{\varepsilon|y|} + 2\ln 2 + g_1(2r_0) \\ &+ \varepsilon\frac{\rho}{2r_0}\left\{-\ln\frac{1}{\varepsilon} + \left\{\ln|y| - \ln r_0 - 2\ln 2 - g_1(2r_0) + 1 + 2r_0 g_1'(2r_0)\right\}\right\}. \end{aligned} \tag{A.17}$$

This is precisely (2.5) after some simplifications and by $\eta = -\frac{1}{\ln\varepsilon}$. To prove (A.16), rewrite

$$2g_2(z) = \int_0^1 \left[\frac{2\tau^2-\tau-1}{\tau^2(1-\tau^2)^{3/2}}\exp(-z\tau) + \frac{1}{\tau^2} - (z-1)\frac{1}{\tau}\right] d\tau.$$

Next note that

$$\frac{1}{\tau^2(1-\tau^2)^{3/2}} = \frac{\partial}{\partial\tau}\left(\frac{-1+2\tau^2}{\tau(1-\tau^2)^{1/2}}\right).$$

Integrating by parts, we then obtain

$$2g_2(z) = \int_0^1 \left[\frac{P(\tau)e^{-z\tau}}{\tau(1-\tau^2)^{1/2}} - (z-1)\frac{1}{\tau}\right] d\tau + z - 2, \tag{A.18}$$

where

$$\begin{aligned} P(\tau) &= \left(-1+2\tau^2\right)\left[-4\tau+1+z\left(2\tau^2-\tau-1\right)\right] \\ &= 4z\tau^4 + (-8-2z)\tau^3 + (2-4z)\tau^2 + (z+4)\tau + (z-1). \end{aligned}$$

Next, define

$$f(z) = \int_0^1 \frac{e^{-z\tau}}{(1-\tau^2)^{1/2}} d\tau \tag{A.19}$$

so that (A.18) becomes

$$2g_2 = -4zf'''(z) + (-8-2z)f''(z) - (2-4z)f'(z) + (z+4)\tau + (z-1)g_1(z) + z - 2. \tag{A.20}$$

Now, integrating by parts, we have

$$f'' = -\frac{f'}{z} + f - \frac{1}{z}. \tag{A.21}$$

Substituting (A.21) into (A.20) and simplifying, we obtain

$$2g_2 = -zf + z + (z-1)g_1.$$

Finally, note that $f(z) = -g_1'(z)$ so that (A.16) follows. ∎

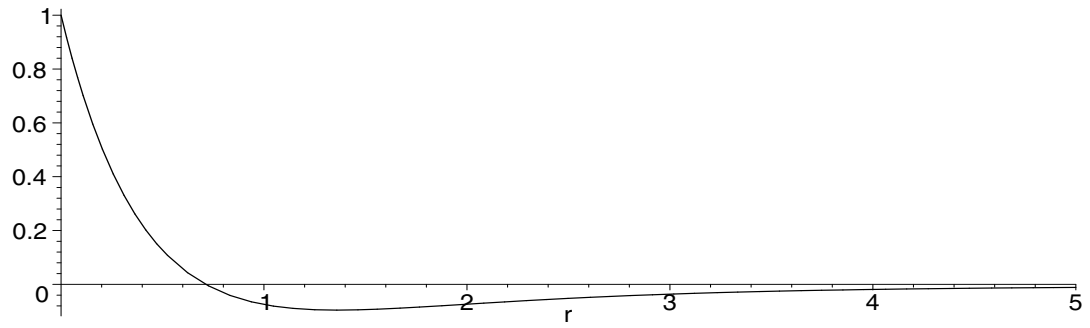

Figure 4. *The plot of the left-hand side of* (1.10).

Appendix B. Existence and uniqueness of the solution to (1.10). Let $f(z)$ be given as in (A.19), and let $g(z) = 1 - zf(z)$. Then the left-hand side of (1.10) is $g(2r_0)$ and is shown in Figure 4. Note that $g(0) = 1$. For large z, we have the asymptotic expansion

$$f(z) = \int_0^1 \frac{e^{-z\tau}}{(1-\tau^2)^{1/2}} d\tau \sim \frac{1}{z} + \frac{1}{z^3} + O(z^{-5}), \quad z \to \infty,$$

so that $g(z) \to 0^-$ as $z \to \infty$. Hence $g(z)$ has at least one root. On the other hand, note that $m - s - 1 > 0$ by assumption (1.7) so that the right-hand side of (1.10) is positive. Moreover, it is clear that $0 \le \frac{\int_0^\infty w^m \left(\int_0^R w^{p+1} t dt\right) RdR}{\left(\int_0^\infty w^m RdR\right)\left(\int_0^\infty w^{p+1} RdR\right)} \le 1$, so that the right-hand side of (1.10) is at most 1 provided that $\frac{1}{2}(m - s - 1) < 1$; the latter follows from (1.7). We conclude that the solution to (1.10) exists provided that (1.7) holds. The uniqueness will be proved if we show that $g(z)$ is decreasing whenever $g(z)$ is positive.

By substituting $f = (1 - g)/z$ into (A.21) we see that $g(z)$ satisfies

$$g'' - \frac{g'}{z} + g\left(\frac{1}{z^2} - 1\right) = \frac{1}{z^2}.$$

Now suppose that $g'(z_0) = 0$ and $g(z_0) > 0$ for some z_0. Then $g''(z_0) = \frac{1}{z_0^2}(1 - g(z_0)) + g(z_0)$. Note that $f(z) > 0$ for all z so that $0 < g(z_0) < 1$. It then follows that $g''(z_0) > 0$. We conclude that $g(z)$ has no maximum if $g(z) > 0$. On the other hand, $g(z) \to 0$ as $z \to \infty$ and $g(0) = 1$. It follows that $g(z)$ is decreasing whenever $g(z)$ is positive. This concludes the proof of the uniqueness of r_0 satisfying (1.10).

Acknowledgments. We are grateful to the anonymous referees for their very careful reading and thoughtful, detailed comments that helped to improve the paper significantly. T. Kolokolnikov is grateful to T.I.M.S., National Taiwan University, for their hospitality and support during the writing of this paper.

REFERENCES

[1] B. P. Anderson, P. C. Haljan, C. A. Regal, D. L. Feder, L. A. Collins, C. W. Clark, and E. A. Cornell, *Watching dark solitons decay into vortex rings in a Bose-Einstein condensate*, Phys. Rev. Lett., 86 (2001), pp. 2926–2929.

[2] G. K. Batchelor, *An Introduction to Fluid Dynamics*, Cambridge University Press, Cambridge, UK, 1967.
[3] A. Doelman, R. A. Gardner, and T. Kaper, *A stability index analysis of 1-D patterns of the Gray Scott model*, Mem. Amer. Math. Soc., 155 (737) (2002).
[4] A. Doelman, T. J. Kaper, and P. Zegeling, *Pattern formation in the one-dimensional Gray-Scott model*, Nonlinearity, 10 (1997), pp. 523–563.
[5] A. Doelman and T. J. Kaper, *Semistrong pulse interactions in a class of coupled reaction-diffusion equations*, SIAM J. Appl. Dyn. Syst., 2 (2003), pp. 53–96.
[6] D. Iron, M. J. Ward, and J. Wei, *The stability of spike solutions to the one-dimensional Gierer-Meinhardt model*, Phys. D, 50 (2001), pp. 25–62.
[7] FlexPDE, http://www.pdesolutions.com.
[8] A. Gierer and H. Meinhardt, *A theory of biological pattern formation*, Kybernetik (Berlin), 12 (1972), pp. 30–39.
[9] T. Kolokolnikov and J. Wei, *Positive clustered layered solutions for the Gierer-Meinhardt system*, J. Differential Equations, 245 (2008), pp. 964–993.
[10] T. Kolokolnikov and J. Wei, *On ring-like solutions for the Gray-Scott model: Existence, instability and self-replicating rings*, European J. Appl. Math., 16 (2005), pp. 201–237.
[11] T. Kolokolnikov, M. J. Ward, and J. Wei, *The existence and stability of spike equilibria in the one-dimensional Gray-Scott model: The low feed rate regime*, Stud. Appl. Math., 115 (2005), pp. 21–71.
[12] T. Kolokolnikov and M. J. Ward, *Reduced wave Green's functions and their effect on the dynamics of a spike for the Gierer-Meinhardt model*, European J. Appl. Math., 14 (2003), pp. 513–545.
[13] A. Malevanets and R. Kapral, *Links, knots, and knotted labyrinths in bistable systems*, Phys. Rev. Lett., 77 (1996), pp. 767–770.
[14] A Malevanets and R. Kapral, *Reactive lattice gas model for FitzHugh-Nagumo dynamics*, Nonlinear Science Today, September (1997).
[15] H. Meinhardt, *Models of Biological Pattern Formation*, Academic Press, London, 1982.
[16] H. Meinhardt, *The Algorithmic Beauty of Sea Shells*, 2nd ed., Springer, Berlin, Heidelberg, 1998.
[17] D. S. Morgan and T. J. Kaper, *Axisymmetric ring solutions of the 2-D Gray-Scott model and their destabilization into spots*, Phys. D, 192 (2004), pp. 33–62.
[18] C. B. Muratov and V. V. Osipov, *Static spike autosolitons in the Gray-Scott model*, J. Phys. A, 33 (2000), pp. 8893–8916.
[19] J. Murray, *Mathematical Biology.* II. *Spatial Models and Biomedical Applications*, 3rd ed., Springer-Verlag, New York, 2003.
[20] W.-M. Ni and J. Wei, *On positive solutions concentrating on spheres for the Gierer-Meinhardt system*, J. Differential Equations, 221 (2006), pp. 158–189.
[21] J. E. Pearson, *Complex patterns in a simple system*, Science, 261 (1993), pp. 189–192.
[22] D. J. Pochan, Z. Chen, H. Cui, K. Hales, K. Qi, and K. L. Wooley, *Toroidal triblock copolymer assemblies*, Science, 306 (2004), pp. 94–97.
[23] S. I. Pohozhaev, *Eigenfunctions of the equation* $\Delta u + 2f(u) = 0$, Sov. Math. Doklady, 5 (1965), pp. 1408–1411.
[24] X. Ren and J. Wei, *A toroidal tube solution of a nonlocal geometric problem*, Interfaces Free Bound., to appear.
[25] G. W. Rayfield and F. Reif, *Quantized vortex rings in superfluid helium*, Phys. Rev., 136 (1964), pp. A1194–A1208.
[26] H. van der Ploeg and A. Doelman, *Stability of spatially periodic pulse patterns in a class of singularly perturbed reaction-diffusion equations*, Indiana Univ. Math. J., 54 (2005), pp. 1219–1301.
[27] M. D. van Dyke, *Perturbation Methods in Fluid Mechanics*, Academic Press, New York, 1964.
[28] M. J. Ward, D. McInerney, P. Houston, D. Gavaghan, and P. Maini, *The dynamics and pinning of a spike for a reaction-diffusion system*, SIAM J. Appl. Math., 62 (2002), pp. 1297–1328.
[29] J. Wei, *On single interior spike solutions of the Gierer-Meinhardt system: Uniqueness and spectrum estimate*, European J. Appl. Math., 10 (1999), pp. 353–378.

[30] J. Wei and M. Winter, *On the two-dimensional Gierer–Meinhardt system with strong coupling*, SIAM J. Math. Anal., 30 (1999), pp. 1241–1263.
[31] J. Wei and M. Winter, *On multiple spike solutions for the two-dimensional Gierer-Meinhardt system: The strong coupling case*, J. Differential Equations, 178 (2002), pp. 478–518.
[32] J. Wei and M. Winter, *Spikes for the two-dimensional Gierer-Meinhardt system: The weak coupling case*, J. Nonlinear Sci., 6 (2001), pp. 415–458.